J Neurophysiol 114: 332–340, 2015.
First published May 13, 2015; doi:10.1152/jn.00170.2015.

Graded boosting of synaptic signals by low-threshold voltage-activated calcium conductance

Martín Carbó Tano, María Eugenia Vilarchao, and Lidia Szczupak

Departamento de Fisiología, Biología Molecular y Celular, Facultad de Ciencias Exactas y Naturales, Universidad de Buenos Aires, Buenos Aires, Argentina; and Instituto de Fisiología, Biología Molecular y Neurociencias, Consejo Nacional de Investigaciones Científicas y Tecnológicas, Ciudad Universitaria, Buenos Aires, Argentina

Submitted 18 February 2015; accepted in final form 7 May 2015

Carbó Tano M, Vilarchao ME, Szczupak L. Graded boosting of synaptic signals by low-threshold voltage-activated calcium conductance. *J Neurophysiol* 114: 332–340, 2015. First published May 13, 2015; doi:10.1152/jn.00170.2015.—Low-threshold voltage-activated calcium conductances (LT-VACCs) play a substantial role in shaping the electrophysiological attributes of neurites. We have investigated how these conductances affect synaptic integration in a premotor nonspiking (NS) neuron of the leech nervous system. These cells exhibit an extensive neuritic tree, do not fire Na^+-dependent spikes, but express an LT-VACC that was sensitive to 250 μM Ni^{2+} and 100 μM NNC 55-0396 (NNC). NS neurons responded to excitation of mechanosensory pressure neurons with depolarizing responses for which amplitude was a linear function of the presynaptic firing frequency. NNC decreased these synaptic responses and abolished the concomitant widespread Ca^{2+} signals. Coherent with the interpretation that the LT-VACC amplified signals at the postsynaptic level, this conductance also amplified the responses of NS neurons to direct injection of sinusoidal current. Synaptic amplification thus is achieved via a positive feedback in which depolarizing signals activate an LT-VACC that, in turn, boosts these signals. The wide distribution of LT-VACC could support the active propagation of depolarizing signals, turning the complex NS neuritic tree into a relatively compact electrical compartment.

calcium conductance; synaptic amplification; nonspiking; dendritic integration; window current

THE NEURITIC TREE IS THE CELLULAR domain at which neurons receive, integrate, and process synaptic inputs, and therefore it is a major determinant of their input/output functions (London and Hausser 2005; Magee 2000). In previous decades, it became clear that dendrites do not rely purely on their passive membrane properties but are supplied with voltage-activated conductances that affect their processing capabilities (Reyes 2001; Yuste and Tank 1996). Among these conductances, low-threshold voltage-activated calcium conductances (LT-VACCs) play a substantial role in shaping the biophysical attributes of neurites (Huguenard 1996), suggesting their involvement in synaptic processing. Synaptic stimulation or focal subthreshold depolarization activate calcium conductances in the dendritic arbor of a variety of neurons (Egger et al. 2005; Eilers et al. 1995; Errington et al. 2010; Ivanov and Calabrese 2006; Laurent et al. 1993; Schiller et al. 1997; Wessel et al. 1999; Yang et al. 2013; Yuste and Denk 1995). However, it is not known to what extent the activation of LT-VACCs shapes the synaptic responses that gave rise to them, influencing their magnitude, dynamics, and propagation.

This question has been addressed in the premotor nonspiking (NS) neuron of the leech nervous system. NS neurons do not fire Na^+-dependent spikes but express an LT-VACC that is activated at around −55 mV (Rela et al. 2009). These neurons are at the center of a recurrent inhibitory circuit that modulates motor output in this annelid (Szczupak 2014). There is one pair of NS neurons per leech midbody ganglion that extend broad neuritic trees in the ganglionic neuropil (see Fig. 3*A*) and are connected through chemical and electrical synapses to all of the motoneurons in the corresponding segment (Rela and Szczupak 2003; Rodriguez et al. 2012; Wadepuhl 1989).

Calcium imaging studies have shown that this LT-VACC is distributed throughout the main branches and is activated by synaptic responses evoked by stimulation of pressure-sensitive (P) neurons (Yang et al. 2013). The resulting Ca^{2+} signals are a graded function of the electrophysiological synaptic responses and spread throughout the neuritic tree with no major attenuation. Thus NS neurons represent an interesting case where synaptically evoked Ca^{2+} signals are a graded function of synaptic inputs but spread globally. The goal of the present investigation is to learn whether this conductance shapes synaptic responses of NS neurons.

The results presented here indicate that LT-VACC amplified the responses to synaptic inputs. This boosting was achieved in a graded manner, and the amplified signal preserved a linear relationship with the firing frequency of the presynaptic neuron.

MATERIALS AND METHODS

Biological preparation. Hirudo sp., weighing 2–5 g, were obtained from a commercial supplier (Leeches USA, Westbury, NY) and maintained at 15°C in artificial pond water. The animals were not fed for at least 1 mo before dissection. The leech nervous system is composed of 21 midbody ganglia, aligned between a head and a tail brain. Each midbody ganglion innervates 1 body segment and contains all of the corresponding sensory and motor neurons (Muller et al. 1981). Individual midbody ganglia were dissected out of the animal and pinned to Sylgard (Dow Corning) in a recording chamber filled with normal saline at room temperature. The sheath covering the ganglion was dissected away, leaving the neuronal cell bodies exposed to the external solution.

Solutions. The ganglia were bathed in standard saline solution with the following composition (in mM): 115 NaCl, 4 KCl, 1.8 $CaCl_2$, 1 $MgCl_2$, and 5.4 HEPES, pH 7.4. Amiloride was purchased from Sigma-Aldrich and NNC 55-0396 dihydrochloride (NNC) from Tocris Bioscience.

Address for reprint requests and other correspondence: L. Szczupak, FBMC-FCEN-UBA, IFIBYNE-CONICET, Ciudad Universitaria, Pabellón II, Piso 2, 1059 Buenos Aires, Argentina (e-mail: szczupak@retina.ar).

Electrophysiological recordings. Microelectrodes were pulled from borosilicate capillary tubing (A-M Systems) using a P-97 Flaming/Brown horizontal puller (Sutter Instrument) and filled with 3 M potassium acetate solution. The recording electrode was also used, where indicated, to apply square pulses or sinusoidal current injections. Electrodes with resistance of 20–30 MΩ were connected to an Axoclamp 2B amplifier (Molecular Devices) operating in current-clamp configuration (with balanced bridge electrodes) or, when stated, in discontinuous current clamp. The recordings were digitized using a Digidata 1320 interface and acquired using Clampex protocols (pCLAMP 9.2; Molecular Devices) at sampling frequencies of 5 kHz. The NS and the mechanosensory P neurons were identified by their location, size, and electrophysiological properties (Muller et al. 1981; Wadepuhl 1989). To activate the P-NS synaptic interaction, P cells were excited by the injection of trains of 5-ms current pulses (2–4 nA) where each pulse evoked a single spike.

Calcium imaging. NS neurons were filled with the calcium-sensitive fluorescent probe Oregon Green 488 BAPTA-1 (OG-1; Invitrogen, Molecular Probes). OG-1 was diluted in 100 mM potassium acetate solution to a final concentration of 3.4 mM and loaded by iontophoresis through an intracellular electrode into the soma. The loading protocol consisted of a series of pulses (0.2 nA for 100 ms followed by −6 nA for 500 ms) that was repeated at 1 Hz for 15 min. The indicator was allowed to diffuse at room temperature for 90 min, changing the saline solution bathing the ganglion every 30 min.

Images of loaded neurons were acquired using a FV1000 confocal system equipped with an argon laser (488 nm; Olympus, Nagano, Japan) through a ×20 water-immersion objective (numerical aperture 0.5). Excitation and emission wavelengths were separated with a dichroic mirror (DM405/488), and emitted light was filtered through a BA505IF filter. Frames formed by 256 × 256 pixels, at a resolution of 2.5 × 2.5 μm^2, were acquired at 2.2 Hz. The pinhole aperture was set at 300 μm. The focal plane exhibiting the most complete view of the NS structure was chosen, and the photomultiplier (PMT) voltage was adjusted to get most of the neuron pixels within 7–60% dynamic range of the PMT. Optical and electrophysiological data acquisition were synchronized. The fluorescence signal was quantified by measuring the mean relative fluorescence change for manually selected regions of interest (ROIs). Four ROIs of 50 × 50 μm were located at the four main branches of NS neurons. Relative fluorescence changes were calculated as $\Delta F/F = [F(t) - F_0]/F_0 \times 100$, where F_0 (average of 10 frames previous to the stimulus) is the baseline fluorescence intensity and $F(t)$ the fluorescence measured at time t during the experiment. Background fluorescence was measured in an equivalent region of the focal plane, away from the cell recorded from. Changes in fluorescence that resulted from bleaching were negligible at the moment of stimulation and needed no correction for analyzing the Ca^{2+} signals (Yang et al. 2013).

Data analysis. The electrophysiological recordings were analyzed using Clampfit software version 10.4 (Molecular Devices), the images were analyzed using Fiji (Schindelin et al. 2012), and the resulting data were analyzed using R (R Core Team 2014) and RStudio (version 0.98.1091; RStudio 2012).

The amplitude of rebound responses evoked by negative current pulses was measured from baseline membrane potential of the NS neurons ($V_{m_{NS}}$; before the pulse) to the peak value developed after the return from the hyperpolarizing response. The amplitude of synaptic responses was measured as the time integral (area) of the response during 2 s following the onset of the stimulus, divided by this period.

Statistical tests and their P value are indicated in RESULTS and figure legends. $P < 0.05$ was chosen as the level of statistical difference. Data are presented as means ± standard error of the mean, and n indicates the number of independent observations.

RESULTS

Pharmacological profile of the LT-VACC of NS neurons. To analyze the role played by LT-VACCs in synaptic integration, it is necessary to count on specific blockers devoid of any effect on the high-threshold VACCs that participate in synaptic transmission. The effects of three pharmacological agents known as T-type Ca^{2+} channel blockers were studied: amiloride (Huguenard and Prince 1992; Tang et al. 1988), Ni^{2+} (Huguenard and Prince 1992; Lee et al. 1999; Regan 1991), and NNC, a structural analog of mibefradil (Huang et al. 2004; Johnston and Delaney 2010).

In an initial screen, we tested how these agents affected the LT-VACC underlying the low-threshold spike evoked by hyperpolarizing pulses (Fig. 1), as this event is a robust expression of this conductance in NS neurons (Rela et al. 2009). To this end, NS neurons at their resting potential (−42 ± 0.5 mV, $n = 10$) were subjected to a hyperpolarizing current pulse (−8 nA, 2 s). On the return from the hyperpolarization, a low-threshold spike was elicited (Fig. 1). Amiloride (300 μM) had no evident effect ($n = 2$) on the normal development of low-threshold calcium spikes in NS neurons (Fig. 1*A*). Ni^{2+}, at a 250 μM concentration, produced a significant reversible reduction of the amplitude of low-threshold calcium spikes (Fig. 1, *Bi* and *Bii*), whereas lower concentrations (100 and 150 μM, $n = 3$ and 5, respectively) showed no effect (data not shown). To test the influence of pharmacological agents on leech synaptic transmission, we tested their effect on the interaction between the mechanosensory P cells and the serotonergic Retzius (Rz) neurons: excitation of P cells evokes excitatory responses in Rz neurons (Szczupak and Kristan 1995; Wittenberg et al. 1990). Figure 1*Biii* shows the excitatory response of a Rz neuron to a train of 6 spikes (15 Hz) in the P cell. In the presence of 250 μM Ni^{2+}, P cells manifested an increase in their excitability, and the cell continued firing beyond the experimental stimulation, causing a prolonged Rz response. Similar responses were observed in 5/12 cases (pairs of neurons). In 5/12 cases, Ni^{2+} also caused the hyperexcitability of Rz cells, which exhibited a larger response than in control condition, even when P cells did not increase their excitability. Blockade of the LT-VACC is not expected to increase the excitability of neurons, and thus we interpret that 250 μM Ni^{2+} also affected other conductances in P and Rz neurons.

Perfusion with NNC (100 μM) drastically diminished the amplitude of low-threshold calcium spikes (Fig. 1, *Ci* and *Cii*). It was reported that the binding site of this drug is within the membrane or intracellular domains of T-type channels, and therefore its effect cannot be reversed on washout (Li et al. 2005). The low-threshold calcium spike developed by NS neurons is a graded phenomenon for which amplitude and time to peak varies with the magnitude of the hyperpolarizing steps used to elicit it (Rela et al. 2009). NNC strongly diminished the rebound responses of NS neurons elicited by a series of hyperpolarizing steps (−1 to −10 nA, 2 s) at any of its graded manifestations (Fig. 1*Ciii*) and exhibited no effect on the P-Rz interaction (Fig. 1*Civ* and in other 2 pairs).

The results indicate that the LT-VACC underlying the rebound response of NS neurons was sensitive to Ni^{2+} and NNC, but the latter was considered a most suitable pharmacological tool to examine the role of this conductance in synaptic integration because it showed a more specific effect on LT-VACC.

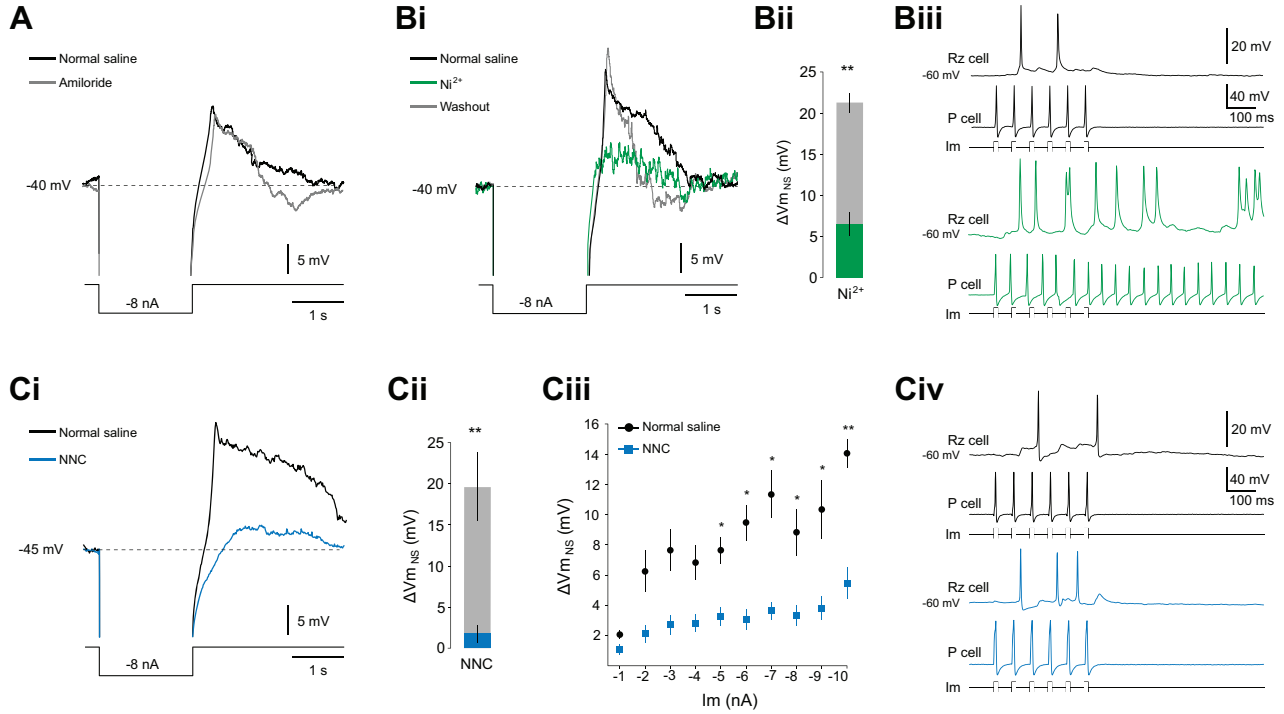

Fig. 1. Pharmacological profile of the low-threshold calcium spike. *A*: representative responses of a nonspiking (NS) neuron to the injection of −8-nA current pulses (2 s) in normal saline and after 10-min perfusion with a solution containing 300 μM amiloride. In this and the rest of the figures, the number on the left of the traces indicates the baseline membrane potential. *Bi*: as in *A*, before and after 10 min in 250 μM Ni^{2+} and after 20-min washout in normal saline. *Bii*: the gray and green bars show the mean rebound response amplitude before and after 10-min perfusion with 250 μM Ni^{2+}, respectively [$n = 8$; paired t-test: $t_{(1)} = 17.6$, $^{**}P < 0.001$]. $\Delta V_{m_{NS}}$, change in the membrane potential of the NS neurons. *Biii*: representative responses of a Retzius (Rz) cell to intracellular stimulation of pressure-sensitive (P) cells in normal saline and after 10-min perfusion with 250 μM Ni^{2+}. P cells fired a train of 6 action potentials at 20 Hz in both conditions. I_m, square current pulse. *Ci*: as in *Bi*, before and after 20 min in 100 μM NNC 55-0396 (NNC). *Cii*: as in *Bii*, for NNC. The gray and blue bars show the rebound amplitude before and after 20-min perfusion with NNC, respectively [$n = 8$; paired t-test: $t_{(1)} = 17.6$, $^{**}P < 0.001$]. *Ciii*: average peak amplitude of the rebound response to successive 2-s hyperpolarizing current pulses of increasing amplitude (−1 to −10 nA) in normal saline and in NNC [$n = 5$; 2-way ANOVA: $F_{(1,9)} = 2.1$, $P < 0.05$, and Tukey honestly significant difference (HSD): $^{**}P < 0.001$ and $^{*}P < 0.05$]. *Civ*: as in *Biii* but for 100 μM NNC.

NS synaptic responses are boosted by the LT-VACC. To evaluate the contribution of the LT-VACC on synaptically evoked responses in NS neurons, we studied the effect of NNC on the interaction between mechanosensory P and NS neurons. Excitation of these sensory neurons evokes phasic depolarizing potentials superimposed on a tonic hyperpolarization (Marín Burgin and Szczupak 2000). Both phases are mediated by an interneuronal layer.

Figure 2*A* shows NS responses evoked by stimulation of a P cell that fired 1-s trains of spikes at different frequencies (10–25 Hz). To minimize the expression of the hyperpolarizing component of these responses, the $V_{m_{NS}}$ was set at −60 mV, close to the reversal potential of this component and below the activation threshold of LT-VACC in these cells. The results obtained in control conditions show that the NS neurons exhibited a barrage of depolarizing bouts surmounted on an underlying steady depolarization. The amplitude of these responses increased as a function of the firing frequency of the presynaptic cells. On perfusion with 100 μM NNC for 20 min, the NS responses markedly decreased (Fig. 2*A*). Because the effect of NNC cannot be washed out, we tested the specificity of NNC effect in a separate set of P-NS pairs that were incubated in normal saline for 20 min.

Figure 2*B* shows the three experimental control data sets that result from our protocol: the responses before the application of NNC (NNC-0min) and the responses at 0 and 20 min of the sets perfused only with normal saline (N-0min and N-20min) plotted as a function of the firing frequency of P cells. The results indicate that the mean synaptic amplitude increased linearly with the presynaptic firing frequency and rule out any effect of incubation time on the responses. Figure 2*C* compares the results obtained before and after the application of NNC, revealing that blockade of the LT-VACC decreased the responses at all stimulation frequencies.

Plotting the amplitude of the postsynaptic responses obtained in control conditions as a function of the amplitude measured in NNC reveals a linear relationship between these two variables (Fig. 2*C*, *inset*) suggesting that the NNC-sensitive conductance amplified the synaptic signal in a graded manner. In other words, the activation of the LT-VACC was a function of the amplitude of the postsynaptic signal and thus boosted it proportionally.

It has been shown that synaptically evoked responses cause an increase in the $[Ca^{2+}]_i$ of NS neurons for which magnitude is a linear function of the amplitude of $\Delta V_{m_{NS}}$ and that these Ca^{2+} signals exhibit a relatively constant magnitude along the neuronal branches (Yang et al. 2013). These data were interpreted as an indication that the LT-VACC is distributed throughout NS branches. To evaluate this hypothesis further, we analyzed the effect of NNC on synaptically evoked Ca^{2+} signals.

Figure 3*A* shows a representative image of an NS neuron that was filled with a fluorescent marker that reveals the

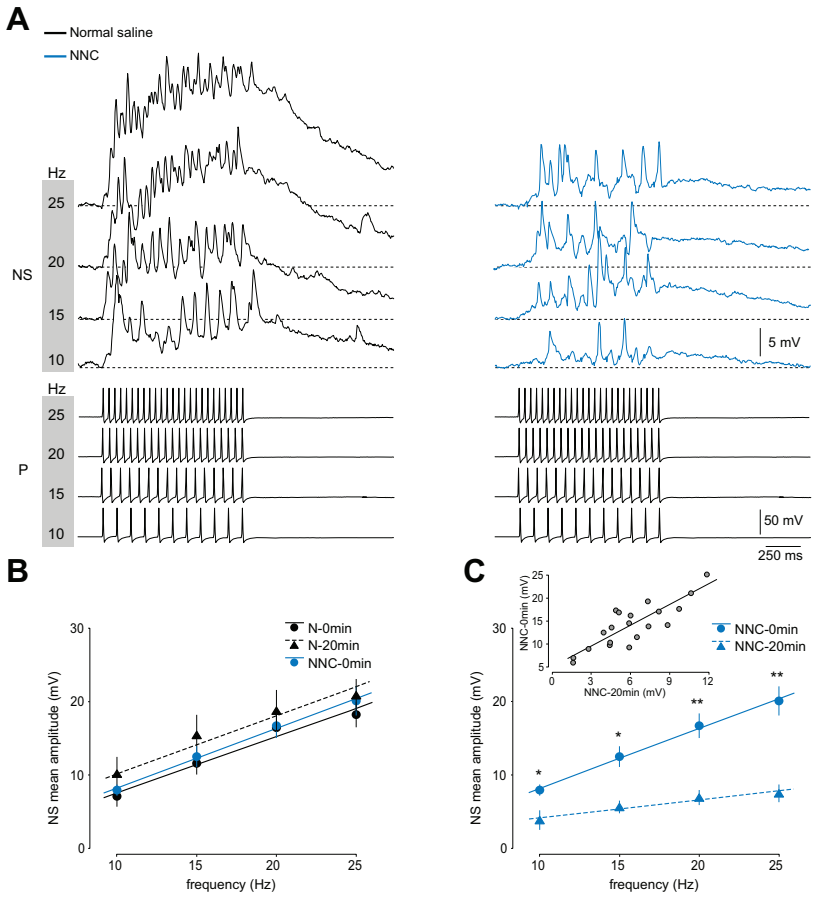

Fig. 2. The low-threshold voltage-activated calcium conductance (LT-VACC) amplifies the synaptic responses of NS neurons. *A*: representative synaptic responses of an NS neuron to stimulation of a P cell with trains of suprathreshold pulses at different frequencies (indicated on the left). The recordings were performed in normal saline (*left*) and after 20-min perfusion with a solution containing 100 μM NNC (*right*). *B*: mean amplitude of NS responses as function of the P cell stimulation frequency in 3 control conditions: in normal saline at *time 0* (N-0min; $n = 5$) and after 20-min perfusion in this solution (N-20min; $n = 5$) and before perfusion with NNC (NNC-0min; $n = 5$). Lines represent the linear regression of each group: solid black line for N-0min (slope 0.7, $r^2 = 0.954$, $P < 0.001$); black dashed line for N-20min (slope 0.8, $r^2 = 0.99$, $P < 0.001$); and solid blue line for NNC-0min (slope 0.81, $r^2 = 0.99$, $P < 0.01$). *C*: as in *B* but comparing the response of NS neurons before and after 20-min perfusion with 100 μM NNC [NNC-20min; $n = 5$; 2-way ANOVA, NNC-0min vs. NNC-20min: $F_{(1,32)} = 3.75$, $P < 0.05$, and Tukey HSD: $^{**}P < 0.001$ and $^{*}P < 0.05$]. The blue dashed line represents the linear regression of NNC-20min (slope 0.34, $r^2 = 0.92$, $P < 0.001$). The *inset* shows the relationship between the responses of NNC-0min and NNC-20min. The line represents the linear regression (slope 1.49, $r^2 = 0.72$, $P < 0.001$).

anatomy of the neuron and Fig. 3*B* the image of another NS loaded with Oregon Green during its response to a P cell stimulation. Changes in fluorescence were evaluated in four ROIs encompassing segments of the four main branches of the cell (Fig. 3*B*, boxed areas 1–4). With $V_{m_{NS}}$ set at −60 mV, P cell stimulation elicited depolarizing potentials in the NS soma (Fig. 3*Ci*) that were accompanied by strong ΔF/F signals in the four main branches of the cell (Fig. 3*Cii*). NNC caused a marked decrease in the amplitude of the electrophysiological signal measured at the soma and of the ΔF/F signals throughout the neuron (Fig. 3, *C–E*).

These data indicate that the LT-VACC is distributed throughout the NS neuritic tree and its activation by synaptic inputs can be responsible for their amplification along the NS branches, supporting an active propagation of these signals. The activation of this NNC-sensitive Ca^{2+} signal is a graded function of the amplitude of the synaptic response (Yang et al. 2013), which is coherent with the graded amplification shown in Fig. 2.

Because the P-NS connection is not direct but involves an interneuronal layer (Marín Burgin and Szczupak 2000), it is also possible that the observed effects were due to the influence of NNC on this layer. Unfortunately, this cellular component has not been identified yet, and therefore we cannot test this possibility in a direct way. Instead, we analyzed the effect of NNC on the responses to direct stimulation of NS neurons.

The responsiveness to depolarizing sinusoidal current is amplified by the LT-VACC. If the NNC-sensitive amplification of synaptic signals was due to the activation of LT-VACC, one expects NNC to produce a similar effect when NS neurons are stimulated by current injection. To represent the dynamic characteristics of synaptic inputs, we tested the effect of NNC when NS neurons were stimulated with sinusoidal current at 30 Hz. This frequency was chosen based on the numbers of $V_{m_{NS}}$ peaks per time unit measured in experiments where we analyzed the responses of NS neurons to P cell stimulation at 20 Hz (see Fig. 2*A*; 31 ± 1 Hz).

Figure 4*A* shows a representative example of NS responses to a 30-Hz sinusoidal current injection (2 nA, 400 ms) in normal saline and in NNC. In both conditions $V_{m_{NS}}$ followed the dynamics imposed by the sinusoidal current, but in normal saline successive cycles evoked voltage bouts surmounted on an underlying steady depolarization that was strongly diminished under NNC treatment. Noticeably, the effect of NNC on responses to sinusoidal current exhibited a general resemblance to that on synaptic responses (Fig. 2*A*).

To quantify the effect, we measured the amplitude of the first and the last cycle in each condition. The amplitude of the response to the first cycle was, on average, unaffected by the presence of NNC (Fig. 4*Bi*). However, Fig. 4*Bii* shows that the degree of NNC effect on the first cycle depended on the $V_{m_{NS}}$ achieved at its peak by each cell. When the first current cycle shifted $V_{m_{NS}}$ to values more positive than −50 mV, NNC caused a decrease in $\Delta V_{m_{NS}}$ that was not observed at more negative potentials. Since the threshold of LT-VACC in NS neurons was around −55 mV (Rela et al. 2009), this observation further suggests that boosting of the first cycle, when it occurred, depended on the activation of this conductance. In the course of the

sinusoidal stimulation, $V_{m_{NS}}$ increased, and the amplitude measured at the peak of the last cycle was significantly larger than that of the first and was drastically diminished by NNC (Fig. 4, *A* and *Bi*).

To rule out a nonspecific action of NNC, we analyzed its effect on responses evoked by injection of negative sinusoidal current (that is not supposed to activate VACCs). Figure 4*C* illustrates the marked overlap of the responses to this stimulation in both conditions. The amplitudes of the first and last cycle were highly similar in control and NNC saline (Fig. 4*D*). These control experiments indicate that the effect of NNC on positive sinusoidal current was due to its specific effect on the LT-VACC.

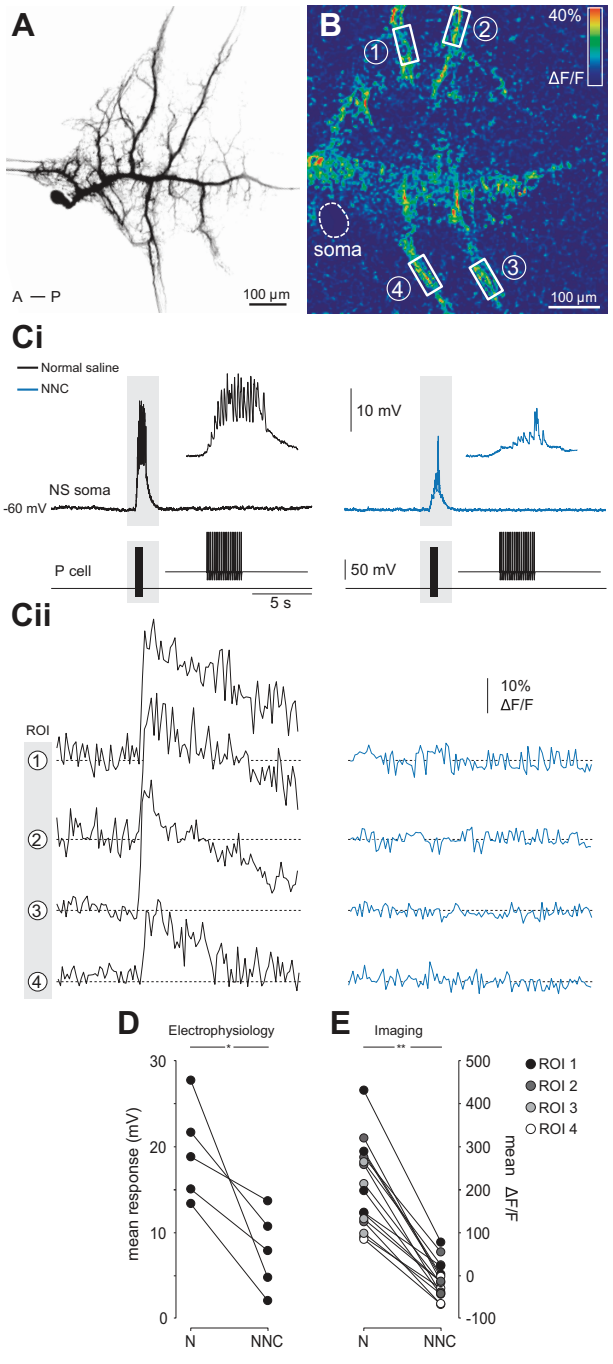

Fig. 3. Calcium transients evoked by synaptic signals are blocked by NNC. *A*: projected confocal *z*-scan of a midbody ganglion where 1 NS neuron was filled with rhodamine dextran (3 kDa). The anterior-posterior (A – P) direction is indicated. The image is formed by the superposition of 15 focal planes taken at 1-μm intervals. *B*: confocal plane of a midbody ganglion where 1 NS neuron was filled with Oregon Green 488 BAPTA-1 (OG-1). The image was taken at 600 ms from the onset of P cell stimulation (1-s spike train at 20 Hz). The fluorescence change is expressed in a color-code scale indicated to the right. Four regions of interest (ROIs) are enclosed in white line boxes. *Ci*: electrophysiological recordings of NS and P cells in normal saline and NNC as the sensory neurons were stimulated as stated above. The *insets* show expanded views of the segments enclosed in the gray boxes. *Cii*: ΔF/F signals evoked by the signals shown in *Ci* in each ROI in normal saline (N) and after perfusion with a solution containing NNC. *D*: time integral of the electrophysiological response of the NS cell to P stimulation in normal saline and NNC. Each dot corresponds to 1 cell [$n = 5$; paired *t*-test, $t_{(4)} = 3.9$, $^*P < 0.05$]. *E*: time integral of the ΔF/F. The 4 ROIs of each cell (identified by the hues on the right) for each of the cells measured in *D* [$n = 25$; paired *t*-test, $t_{(15)} = 5.6$, $^{**}P < 0.001$].

At the end of positive sinusoidal current injection, $V_{m_{NS}}$ returned to baseline following a slow time course. This "voltage tail" was probably due to the slow deactivation of the LT-VACC activated during the sinusoidal current injection (Fox et al. 1987; Huguenard and Prince 1992; Kozlov et al. 1999). NNC trimmed the voltage tails (Fig. 4*E*), supporting this hypothesis. The voltage tails evoked by negative sinusoidal current injection were unaffected by NNC (Fig. 4*E*), their magnitudes were similar to those exhibited by positive sinusoidal currents in NNC, and the voltage tails probably correspond to the passive properties of the NS neurons.

The results indicate that LT-VACC amplified depolarizing signals impinging on NS. Although we cannot rule out an effect of NNC on the interneurons mediating the P-NS pathway, comparison of the results described in Figs. 2 and 4 supports the interpretation that the synaptic responses were amplified, to a large extent, by the activation of LT-VACC in NS neurons.

The LT-VACC supported signal propagation. The effect of LT-VACC on the magnitude of synaptic responses could be due to two not mutually exclusive causes: *1*) signal amplification at its site of origin; and *2*) active propagation from the input to the recording site. Although the results from the previous section suggest that this conductance amplifies depolarizing responses, the second cause can still play a role in synaptic integration. The fact that NNC-sensitive Ca^{2+} signals are distributed along different branches (Fig. 3) indicates that LT-VACC could be the substrate for signal propagation. To test this hypothesis in a more direct way, we took advantage of the fact that the contralateral pair of NS neurons in each ganglion are electrically coupled through ohmic conductances (Fig. 5*A*) with a relatively high coupling coefficient of ~0.25 (Fig. 5*B*). The two somata present convenient recording sites where to monitor the spatial spread of electrical signals.

In dual recordings, a series of hyperpolarizing pulses were injected in one NS producing a graded family of low-threshold calcium spikes in both NS cells. The responses of both NS neurons were undistinguishable at any of the graded expressions of the rebound responses (Fig. 5, *C–E*). This observation further supports the view that the LT-VACC underlying these responses are widely distributed throughout the NS neuritic tree.

To evaluate whether LT-VACC is involved in the propagation of dynamic depolarizing signals, 30-Hz sinusoidal current

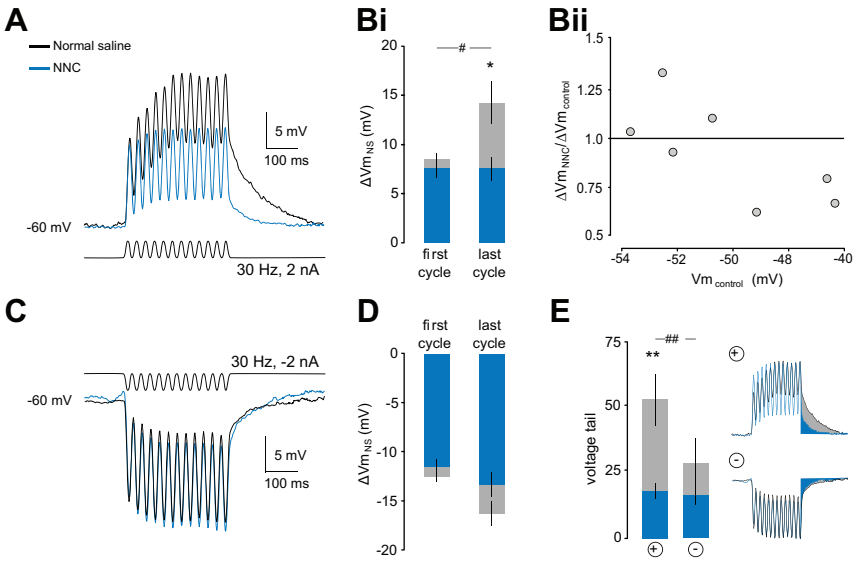

Fig. 4. Blocking LT-VACC had a pronounced effect on NS responses to dynamic stimulation. *A*: representative responses of an NS neuron to the injection of a 2-nA sinusoidal current injection at 30 Hz in normal saline and after 10-min perfusion with NNC. The experiments were performed in discontinuous current clamp (DCC) mode. *Bi*: the bars indicate the average amplitude of the 1st and last cycle in normal saline and in NNC [$n = 7$; 2-way ANOVA, $F_{(1,12)} = 4.2$, $P < 0.05$; Tukey HSD, $^{*}P < 0.05$ for the comparison between responses in normal saline and in NNC and $\#P < 0.05$ for the comparison between the 1st and last cycle in normal saline]. *Bii*: the plot shows the relative amplitude of the 1st cycle after NNC [$\Delta V_{m_{NNC}}/\Delta V_{m_{control}}$] as a function of the peak $V_{m_{NS}}$ achieved in normal saline. *C*: as in *A* but for the injection of −2-nA sinusoidal sweeps. *D*: as in *Bi* for negative sinusoidal current injection in normal saline and in NNC [$n = 7$; 2-way ANOVA, $F_{(1,8)} = 4.1$, $P = 0.07$]. *E*: magnitude of the voltage tail measured for positive and negative sinusoidal stimuli in normal saline and in NNC. The *inset* indicates how these measurements were made: the traces (those shown in *A*) were normalized to the amplitude of the last cycle, and the voltage tail was measured as the time integral for 200 ms from the peak of the last cycle [$n = 7$ for positive and $n = 7$ negative current, 2-way ANOVA, $F_{(1,10)} = 9.7$, $P < 0.01$; Tukey HSD, $^{**}P < 0.001$ for the comparison between responses in normal saline and in NNC; $\#\#P < 0.001$ for the comparison between responses to positive and negative stimulation in normal saline].

was injected into the soma of one NS neuron (NS-1), and voltage responses in the driven neuron (NS-1) and in the coupled NS neuron (NS-2) were recorded in normal saline and in NNC (Fig. 5*F*). Although NNC had no effect on the coupling coefficient of NS neurons (Fig. 5*G*), the "effective coupling" for sinusoidal signals, defined as the relationship between the time integral of the response of NS-2 over that of NS-1, was of ~0.7 in normal saline and of ~0.25 in NNC (Fig. 5*H*). These results indicate that when the LT-VACC was blocked, the passive spread of sinusoidal signal from NS-1 to NS-2 matched the coupling coefficient between the neurons (Fig. 5, *B* and *G*). In the presence of LT-VACC, the signal reaching NS-2, relative to the original signal evoked in NS-1, was almost three times larger (Fig. 5*H*). If the effect of LT-VACC was just boosting the signal at the site of origin (NS-1), the effective coupling should not have been affected by NNC and the signal should have been passively attenuated when reaching NS-2, proportional to the size at the site of origin. These results support the view that LT-VACC mediated the active propagation of depolarizing signals along the neuritic tree of NS neurons.

An additional indication that LT-VACC was involved in the propagation of sinusoidal signals was provided by comparing the voltage tails of the signals recorded in both neurons. The voltage tails in NS-1 and NS-2 recordings in normal saline were undistinguishable, and NNC effectively reduced them to a similar magnitude (Fig. 5*I*).

DISCUSSION

LT-VACC amplifies synaptic responses in a graded manner. This study reports a case where synaptic amplification is achieved by virtue of a positive feedback: depolarizing signals activate an LT-VACC that in turn boost these signals. Synaptic stimulation of NS neurons evokes Ca^{2+} signals that are proportional to the amplitude of the electrophysiological response (Yang et al. 2013) and were mediated by an NNC-sensitive LT-VACC (Fig. 3). In turn, the activated LT-VACC caused a graded boosting of synaptic responses. The amplitude of synaptic responses in control conditions was a linear function of the amplitude of these responses when the LT-VACC was blocked (Fig. 2*C*, *inset*). If the amplification mediated by this conductance was sensitive to a threshold $V_{m_{NS}}$ value, beyond which an all-or-none event was triggered, no such linear relationship would have been expected.

Amplification of the responses to synaptic and sinusoidal current stimulation was achieved by the buildup of a steady depolarization (Figs. 2 and 4). This implies that in the course of the dynamic responses at least part of the LT-VACC remained activated. This fits well with the concept of window current associated with LT-VACCs (Crunelli et al. 2005), according to which a steady-state component is originated at the overlap between the activation and inactivation voltage range. Nonetheless, the present results cannot rule out that on top of the LT-VACC effect the amplification could involve a high-threshold VACC or even a persistent Na^{+} conductance.

In the present study, NS neurons were studied as their membrane potential was set below the activation threshold of the LT-VACC (−55 mV). At the resting potential (−40 mV), this conductance was only partially inactivated (Yang et al. 2013), and in this condition NS neurons should retain their ability to boost depolarizing synaptic signals. On the other hand, as indicated in RESULTS, the P-NS interaction includes a

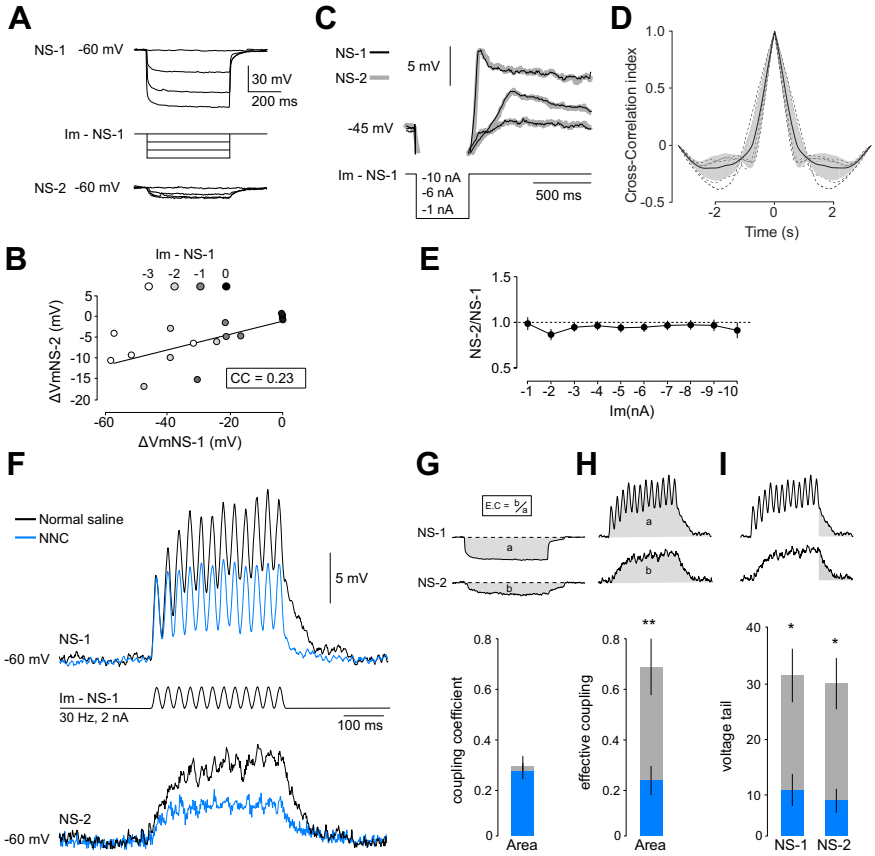

Fig. 5. The LT-VACC supports the propagation of signals between NS neurons. In these experiments, simultaneous recordings from pairs of NS neurons within a ganglion were performed. *A*: representative responses of an NS neuron (NS-1) to the injection of a series of square current pulses (I_m; 0 to −3 nA at 1-nA intervals) in NS-1 while the membrane potential of the contralateral NS neuron (NS-2) was recorded. NS-1 was recorded in DCC mode. *B*: plot of the amplitude of the NS-2 responses as a function of the amplitude of the NS-1 responses. The line presents a linear fit [$n = 4$; $r^2 = 0.82$, $F_{(1,26)} = 121$, $P < 0.05$]. The coupling coefficient (CC) is calculated from the slope of this line (CC = 0.23). The responses to the different current amplitudes are coded in the hues above the graph. *C*: rebound responses of NS-1 (black thin trace) and NS-2 (gray thick trace) to hyperpolarizing current pulses injected in NS-1 (−1, −6, and −10 nA for bottom, middle, and top traces, respectively). Notice that the responses of both cells superpose so well that they cannot be distinguished from each other. *D*: average cross-correlogram (full line) of 6 different pairs of response traces of NS-1 and NS-2 to −8-nA current pulses injected to NS-1. The gray shade represents the 95% confidence interval for the mean cross-correlation index. The dashed lines show each individual cross-correlogram. *E*: relationship between the maximal amplitude recorded in NS-2 over the maximal amplitude recorded in NS-1 in a 1-s period after the end of the current pulses as a function of the current amplitude (−1 to −10 nA; $n = 10$). *F*: representative responses of NS-1 and NS-2 to the injection of a 2-nA sinusoidal current injection at 30 Hz in NS-1 in normal saline and after 10-min perfusion with NNC. *G*: the bars indicate the electrical coupling (E.C) between the NS neurons in normal saline and in NNC measured as the ratio of the time integrals (*b*/*a*; see *top inset*) of a −1-nA square pulse injected to NS-1 [$n = 4$; paired *t*-test, $t_{(3)} = 0.92$, $P = 0.42$]. *H*: the bars indicate the effective coupling between the NS neurons in normal saline and in NNC measured as the ratio of the time integrals [$n = 4$; paired *t*-test, $t_{(3.7)} = 7.1$, $^{**}P < 0.001$]. *I*: the bars indicate the magnitude of the voltage tails in NS-1 and NS-2 in both conditions [$n = 4$; 2-way ANOVA, $F_{(1,12)} = 17.8$, $P < 0.01$; Tukey HSD, $^{*}P < 0.05$] measured as indicated in Fig. 4*E*.

tonic hyperpolarizing component that would naturally hyperpolarize $V_{m_{NS}}$ and thus favor deinactivation of LT-VACC.

LT-VACC could support the active propagation of signals. The distribution of LT-VACC in the neuritic tree sets the scenario for an active propagation of depolarizing signals. That LT-VACC is distributed throughout the NS neuritic tree is supported by two main independent observations: Ca^{2+} signals evoked by low-threshold calcium spikes display a relatively homogeneous amplitude throughout the NS branches (Yang et al. 2013), and low-threshold calcium spikes elicited in one NS reached the contralateral electrically coupled NS neuron with intact characteristics (Fig. 5, *C–E*). We interpret that, when activated at the rebound from a hyperpolarizing signal, the LT-VACC is activated simultaneously at multiple sites, rendering simultaneous responses in both cells. This would not have been expected if LT-VACC was not distributed throughout the entire neuritic tree connecting both somata.

Using sinusoidal current injections, we showed that LT-VACC partially counteracts the effect of passive attenuation of signals that are transmitted from one NS to its coupled contralateral homolog (Fig. 5, *F* and *H*). If the effect of LT-VACC was limited to amplify the signals at their site of origin, no effect on the effective coupling should have been observed. Because NNC had no effect on the coupling itself (Fig. 5*G*), we conclude that activation of LT-VACC supported the active propagation of depolarizing signals from any input site to the rest of the neuritic tree.

It is important to note that, different from what has been observed in response to sinusoidal current injection in one NS, in response to synaptic stimulation the pair of NS neurons display identical signals (Rela and Szczupak 2003). This pattern is probably achieved, as with other coupled neurons in the leech ganglion (Szczupak and Kristan 1995), by the contribution of two factors: *1*) concomitant inputs to and *2*) electrical

transmission in between the bilateral pair of coupled neurons. We propose that, regarding depolarizing signals, the active properties conferred by the distributed LT-VACC contribute to turn the complex neuritic tree of the NS neurons into a relatively compact electrical compartment. Thus, although symmetrical inputs probably play an important role in causing similar responses in both NS neurons, the active properties enhance the ability of the pair of NS neurons to perform as a single unit by boosting and propagating the signals from the site of origin to the rest of the branches (including the 2 somata).

The LT-VACC of NS neurons is analogous to T-type Ca^{2+} conductances. LT-VACC in NS neurons was sensitive to Ni^{2+} and NNC (Fig. 1), a specific blocker of T-type Ca^{2+} conductances in vertebrates (Huang et al. 2004; Li et al. 2005). Thus, given its electrophysiological (Rela et al. 2009) and pharmacological characteristics, the LT-VACC of leech NS neurons can be functional and pharmacologically related to vertebrate (Huguenard 1996; Perez Reyes 2003) and invertebrate (Senatore and Spafford 2010) T-type Ca^{2+} conductances. However, a more detailed biophysical and molecular characterization needs to be performed to classify the LT-VACC of NS neurons.

Calcium conductances influence synaptic integration in a variety of modalities. To our knowledge, the results shown here represent the first description of a neuron in which a voltage-activated conductance in general, and an LT-VACC in particular, produces graded boosting of synaptic signals and supports their active propagation throughout the neuritic tree. In published reports, T-type Ca^{2+} conductance evokes either a local graded amplification of synaptic signals (Urban et al. 1998) or a global all-or-none effect (Egger et al. 2005; Goldberg et al. 2004); alternatively, T-type Ca^{2+} conductances amplified synaptic inputs locally but in a steplike manner (Crandall et al. 2010; Egger et al. 2005; Plotkin et al. 2011; Schiller et al. 1997). These different scenarios should be interpreted on the basis of the physiological role of each neuron.

Possible role of LT-VACC in NS neurons. LT-VACCs have been classically associated with burst firing, which rises on low-threshold calcium spikes (Arbas and Calabrese 1987; Greene et al. 1986; Jahnsen and Llinás 1984a; Pinato and Midtgaard 2003), and to sustain oscillatory activity (Anderson et al. 2012; Bal and McCormick 1993; Jahnsen and Llinás 1984b). In these cases, LT-VACCs operate as a means to reach the threshold of Na^{+}-dependent spikes.

NS neurons do not spike high-threshold spikes, and their electrophysiological performance seems to take place in a graded voltage scale. These premotor cells are linked to motoneurons by chemical and electrical synapses that form a recurrent inhibitory network (Rela and Szczupak 2003; Rodriguez et al. 2009; Szczupak 2014). The NS neurons receive inhibitory inputs from motoneurons by chemical connections and, in addition, exchange information with the motoneurons via electrical connections. Because of the rectifying nature of the electrical junctions between NS and the motoneurons, depolarization of NS deactivates these junctions. When $V_{m_{NS}}$ is more positive than the membrane potential of motoneurons, the gap junction loses conductance. Thus depolarization of NS neurons signals uncoupling, causing a transient halt of the recurrent inhibitory circuit among motoneurons. With regard to the depolarizations elicited by P cells, it is important to note that these mechanosensory cells function as major triggers of motor behaviors in the leech such as swimming and crawling (Kristan 1982). The depolarizing effect of these mechanosensory neurons on NS could cause a synchronized removal of inhibitory transmission among motoneurons at the onset of the execution of motor behaviors. Graded amplification and propagation of depolarizing signals by LT-VACC, as reported here, can modulate the spread of the uncoupling signal throughout the NS neuritic tree, reaching the connection sites with different motoneurons.

ACKNOWLEDGMENTS

We thank Dr. Francisco Urbano for encouraging discussion of the experiments and results and Drs. Violeta Medan and Antonia Marín Burgin for encouraging and critical revision of the present manuscript.

GRANTS

The research has been supported by grants from University of Buenos Aires (UBACYT 2011–2014 20020100100962) and from Agencia Nacional de Promoción Científica y Tecnológica de la República Argentina (PICT 2010-0606) to L. Szczupak.

DISCLOSURES

No conflicts of interest, financial or otherwise, are declared by the authors.

AUTHOR CONTRIBUTIONS

M.C.T. and L.S. conception and design of research; M.C.T. and M.E.V. performed experiments; M.C.T., M.E.V., and L.S. analyzed data; M.C.T., M.E.V., and L.S. interpreted results of experiments; M.C.T. prepared figures; M.C.T. and L.S. drafted manuscript; M.C.T. and L.S. edited and revised manuscript; M.C.T., M.E.V., and L.S. approved final version of manuscript.

REFERENCES

Anderson TM, Abbinanti MD, Peck JH, Gilmour M, Brownstone RM, Masino MA. Low-threshold calcium currents contribute to locomotor-like activity in neonatal mice. *J Neurophysiol* 107: 103–113, 2012.

Arbas EA, Calabrese RL. Ionic conductances underlying the activity of interneurons that control heartbeat in the medicinal leech. *J Neurosci* 7: 3945–3952, 1987.

Bal T, McCormick DA. Mechanisms of oscillatory activity in guinea-pig nucleus reticularis thalami in vitro: a mammalian pacemaker. *J Physiol* 468: 669–691, 1993.

Crandall SR, Govindaiah G, Cox CL. Low-threshold Ca^{2+} current amplifies distal dendritic signaling in thalamic reticular neurons. *J Neurosci* 30: 15419–15429, 2010.

Crunelli V, Toth TI, Cope DW, Blethyn K, Hughes SW. The 'window' T-type calcium current in brain dynamics of different behavioural states. *J Physiol* 562: 121–129, 2005.

Egger V, Svoboda K, Mainen ZF. Dendrodendritic synaptic signals in olfactory bulb granule cells: local spine boosts and global low-threshold spike. *J Neurosci* 25: 3521–3530, 2005.

Eilers J, Augustine GJ, Konnerth A. Subthreshold synaptic Ca^{2+} signalling in fine dendrites and spines of cerebellar Purkinje neurons. *Nature* 373: 155–158, 1995.

Errington AC, Renger JJ, Uebele VN, Crunelli V. State-dependent firing determines intrinsic dendritic Ca^{2+} signaling in thalamocortical neurons. *J Neurosci* 30: 14843–14853, 2010.

Fox AP, Nowycky MC, Tsien RW. Single-channel recordings of three types of calcium channels in chick sensory neurones. *J Physiol* 394: 173–200, 1987.

Goldberg JH, Lacefield CO, Yuste R. Global dendritic calcium spikes in mouse layer 5 low threshold spiking interneurones: implications for control of pyramidal cell bursting. *J Physiol* 558: 465–478, 2004.

Greene RW, Haas HL, McCarley RW. A low threshold calcium spike mediates firing pattern alterations in pontine reticular neurons. *Science* 234: 738–740, 1986.

Hagiwara N, Irisawa H, Kameyama M. Contribution of two types of calcium currents to the pacemaker potentials of rabbit sino-atrial node cells. *J Physiol* 395: 233–253, 1988.

Huang L, Keyser BM, Tagmose TM, Hansen JB, Taylor JT, Zhuang H, Zhang M, Ragsdale DS, Li M. NNC 55-0396 [(1*S*,2*S*)-2-(2-(*N*-[(3-benzimidazol-2-yl)propyl]-*N*-methylamino)ethyl)-6-fluoro-1,2,3,4-tetrahydro-1-isopropyl-2-naphtyl cyclopropanecarboxylate dihydrochloride]: a new selective inhibitor of T-type calcium channels. *J Pharmacol Exp Ther* 309: 193–199, 2004.

Huguenard JR. Low-threshold calcium currents in central nervous system neurons. *Proc Natl Acad Sci USA* 58: 329–348, 1996.

Huguenard JR, Prince DA. A novel T-type current underlies prolonged Ca^{2+}-dependent burst firing in GABAergic neurons of rat thalamic reticular nucleus. *J Neurosci* 12: 3804–3817, 1992.

Ivanov AI, Calabrese RL. Graded inhibitory synaptic transmission between leech interneurons: assessing the roles of two kinetically distinct low-threshold Ca currents. *J Neurophysiol* 96: 218–234, 2006.

Jahnsen H, Llinás R. Electrophysiological properties of guinea-pig thalamic neurones: an in vitro study. *J Physiol* 349: 205–226, 1984a.

Jahnsen H, Llinás R. Ionic basis for the electro-responsiveness and oscillatory properties of guinea-pig thalamic neurones in vitro. *J Physiol* 349: 227–247, 1984b.

Johnston J, Delaney KR. Synaptic activation of T-type Ca^{2+} channels via mGluR activation in the primary dendrite of mitral cells. *J Neurophysiol* 103: 2557–2569, 2010.

Kozlov AS, McKenna F, Lee JH, Cribbs LL, Perez-Reyes E, Feltz A, Lambert RC. Distinct kinetics of cloned T-type Ca^{2+} channels lead to differential Ca^{2+} entry and frequency-dependence during mock action potentials. *Eur J Neurosci* 11: 4149–4158, 1999.

Kristan WB. Behavioural and mechanosensory neurone responses to skin stimulation in leeches. *J Exp Biol* 96: 143–160, 1982.

Laurent G, Seymour-Laurent K, Johnson K. Dendritic excitability and a voltage-gated calcium current in locust nonspiking local interneurons. *J Neurophysiol* 69: 1484–1498, 1993.

Lee JH, Gomora JC, Cribbs LL, Perez-Reyes E. Nickel block of three cloned T-type calcium channels: low concentrations selectively block alpha1H. *Biophys J* 77: 3034–3042, 1999.

Li M, Hansen JB, Huang L, Keyser BM, Taylor JT. Towards selective antagonists of T-type calcium channels: design, characterization and potential applications of NNC 55-0396. *Cardiovasc Drug Rev* 23: 173–196, 2005.

London M, Hausser M. Dendritic computation. *Annu Rev Neurosci* 28: 503–532, 2005.

Magee JC. Dendritic integration of excitatory synaptic input. *Nat Rev Neurosci* 1: 181–190, 2000.

Marín Burgin A, Szczupak L. Processing of sensory signals by a non-spiking neuron in the leech. *J Comp Physiol* 186: 989–997, 2000.

McCobb DP, Best PM, Beam KG. Development alters the expression of calcium currents in chick limb motoneurons. *Neuron* 2: 1633–1643, 1989.

Muller KJ, Nicholls JG, Stent GS. *Neurobiology of the Leech*. Cold Spring Harbor, NY: Cold Spring Harbor Laboratory, 1981.

Perez Reyes E. Molecular physiology of low-voltage-activated T-type calcium channels. *Physiol Rev* 83: 117–161, 2003.

Pinato G, Midtgaard J. Regulation of granule cell excitability by a low-threshold calcium spike in turtle olfactory bulb. *J Neurophysiol* 90: 3341–3351, 2003.

Plotkin JL, Day M, Surmeier DJ. Synaptically driven state transitions in distal dendrites of striatal spiny neurons. *Nat Neurosci* 14: 881–888, 2011.

R Core Team. *R: A Language and Environment for Statistical Computing* (Online). R Foundation for Statistical Computing, Vienna, Austria. http://www.R-project.org/, 2014.

Regan LJ. Voltage-dependent calcium currents in Purkinje cells from rat cerebellar vermis. *J Neurosci* 11: 2259–2269, 1991.

Rela L, Szczupak L. Coactivation of motoneurons regulated by a network combining electrical and chemical synapses. *J Neurosci* 23: 682–692, 2003.

Rela L, Yang SM, Szczupak L. Calcium spikes in a leech nonspiking neuron. *J Comp Physiol* 195: 139–150, 2009.

Reyes A. Influence of dendritic conductances on the input-output properties of neurons. *Annu Rev Neurosci* 24: 653–675, 2001.

Rodriguez MJ, Alvarez RJ, Szczupak L. Effect of a nonspiking neuron on motor patterns of the leech. *J Neurophysiol* 107: 1917–1924, 2012.

Rodriguez MJ, Perez-Etchegoyen CB, Szczupak L. Premotor nonspiking neurons regulate coupling among motoneurons that innervate overlapping muscle fiber population. *J Comp Physiol A* 195: 1351–1432, 2009.

RStudio. *RStudio: Integrated Development Environment for R* (Version 99.9.9). Boston, MA. http://www.rstudio.com/, 2012.

Schiller J, Schiller Y, Stuart G, Sakmann B. Calcium action potentials restricted to distal apical dendrites of rat neocortical pyramidal neurons. *J Physiol* 505: 605–616, 1997.

Schindelin J, Arganda-Carreras I, Frise E, Kaynig V, Longair M, Pietzsch T, Preibisch S, Rueden C, Saalfeld S, Schmid B, Tinevez JY, White DJ, Hartenstein V, Eliceiri K, Tomancak P, Cardona A. Fiji: an open-source platform for biological-image analysis. *Nat Methods* 9: 676–682, 2012.

Senatore A, Spafford JD. Transient and big are key features of an invertebrate T-type channel (LCav3) from the central nervous system of *Lymnaea stagnalis*. *J Biol Chem* 285: 7447–7458, 2010.

Szczupak L. Recurrent inhibition in motor systems, a comparative analysis. *J Physiol (Paris)* 108: 148–154, 2014.

Szczupak L, Kristan WB. Widespread mechanosensory activation of the serotonergic system of the medicinal leech. *J Neurophysiol* 74: 2614–2624, 1995.

Tang CM, Presser F, Morad M. Amiloride selectively blocks the low threshold (T) calcium channel. *Science* 240: 213–215, 1988.

Urban NN, Henze DA, Barrionuevo G. Amplification of perforant-path EPSPs in CA3 pyramidal cells by LVA calcium and sodium channels. *J Neurophysiol* 80: 1558–1561, 1998.

Wadepuhl M. Depression of excitatory motoneurones by a single neurone in the leech central nervous system. *J Exp Biol* 143: 509–527, 1989.

Wessel R, Kristan WB, Kleinfeld D. Dendritic Ca^{2+}-activated K^+ conductances regulate electrical signal propagation in an invertebrate neuron. *J Neurosci* 19: 8319–8326, 1999.

Wittenberg G, Loer CM, Adamo SA, Kristan WB. Segmental specialization of neuronal connectivity in the leech. *J Comp Physiol A* 167: 453–459, 1990.

Yang SM, Vilarchao ME, Rela L, Szczupak L. Wide propagation of graded signals in nonspiking neurons. *J Neurophysiol* 109: 711–720, 2013.

Yuste R, Denk W. Dendritic spines as basic functional units of neuronal integration. *Nature* 375: 682–684, 1995.

Yuste R, Tank DW. Dendritic integration in mammalian neurons, a century after cajal. *Neuron* 16: 701–716, 1996.